Published in final edited form as:

ECS Trans. 2012 ; 41(41): 207–214. doi:10.1149/1.4717978.

Solid State Multinuclear Magnetic Resonance Investigation of Electrolyte Decomposition Products on Lithium Ion Electrodes

J.H.S.R. DeSilva[a,b], **V. Udinwe**[a], **P.J. Sideris**[a], **M. C. Smart**[c], **F.C. Krause**[c], **C. Hwang**[c], **K. A. Smith**[c], and **S. G. Greenbaum**[a,b]

[a]Department of Physics and Astronomy, Hunter College of CUNY, New York, New York 10065, USA

[b]Graduate Center of CUNY, New York, New York, 10016, USA

[c]Jet Propulsion Laboratory, California Institute of Technology, Pasadena, California 91109, USA

Abstract

Solid electrolyte interphase (SEI) formation in lithium ion cells prepared with advanced electrolytes is investigated by solid state multinuclear (^{7}Li, ^{19}F, ^{31}P) magnetic resonance (NMR) measurements of electrode materials harvested from cycled cells subjected to an accelerated aging protocol. The electrolyte composition is varied to include the addition of fluorinated carbonates and triphenyl phosphate (TPP, a flame retardant). In addition to species associated with $LiPF_6$ decomposition, cathode NMR spectra are characterized by the presence of compounds originating from the TPP additive. Substantial amounts of LiF are observed in the anodes as well as compounds originating from the fluorinated carbonates.

Introduction

Lithium-ion batteries consist of a lithiated transition metal oxide as the cathode, a carbonaceous material as the anode and an electrolyte solution of a lithium salt in a mixture of two or more organic solvents, typically carbonates (1). When in contact with liquid electrolytes, lithium (for lithium metal batteries) or lithiated graphite (for lithium ion batteries) are thermodynamically unstable toward the solvents and salts and react to form a passivating film coating that inhibits further corrosion of the anode and allows transport of Li ions between the electrode and electrolyte. This layer, known as SEI (solid electrolyte interphase) formed instantaneously upon contact of the anode with the solution, consists of insoluble and partially soluble reduction products of electrolyte components (1–5). Although the specific nature of the electrochemical reactions occurring on the cathode are different than on the anode, SEI formation is also present at the cathode. The SEI determines the safety, power capability, morphology of lithium deposits, shelf life, and cycle life of the battery. Therefore it is very important to study the nature of the SEI in order to better understand the limits of Li ion battery performance.

Recent safety concerns, especially for large format batteries, have led to the formulation of alternative electrolytes or the introduction of additives. Two particular examples are the use of fluorinated carbonates, which exhibit enhanced electrochemical and thermal stability compared to the traditional non-fluorinated ones (6,7), and fire-retardant additives such as

triphenyl phosphate (TPP) (8,9). As an indicator of the efficacy of these approaches on battery performance and lifetime, it is of interest to investigate the SEI in cells prepared with these advanced electrolytes.

Solid state nuclear magnetic resonance (NMR) has been employed previously to identify the nature of the SEI, including its lithium content, which is related to the irreversible fraction of Li in the cell (10) or in some cases, its composition (11–14). The unique quantitative nature of NMR via the ability to directly integrate peak intensities that represent the bulk response of the sample (as opposed to the surface) provides information that complements other spectroscopic methods such as x-ray-photoelectron spectroscopy and Fourier transform infrared spectroscopy, which provide qualitative chemical speciation information with much less quantitative certainty than NMR (15). In this investigation, multinuclear (^{7}Li, ^{19}F, ^{31}P) solid state magic angle spinning (MAS) NMR studies of SEI formation were performed on both positive $LiNi_{0.8}Co_{0.2}O_2$ and negative graphitic (MCMB) electrode materials harvested from Li ion cells subjected to an accelerated aging protocol

Experimental

To evaluate the various electrolytes, three-electrode spiral rolls of MCMB-(1028)-carbon anodes, $LiNi_{0.80}Co_{0.2}O_2$ cathodes, and lithium reference electrodes were contained in O-ring sealed, glass cells. Two layers of porous polypropylene (Tonen-Setella) separated the two electrodes. The anode electrodes were coated with active material on both sides of the copper substrate and had an active material area of approximately 158 cm^2, corresponding to ~ 16 mg/cm^2. The cathode electrodes were also double sided and coated on aluminum substrate with an active material area of approximately 141 cm^2, corresponding to ~ 19 mg/cm^2. The cathode electrodes (~ 114 μM in thickness) were also double sided with an active material area of approximately 141.1 cm^2, corresponding to ~ 19 mg/cm^2. The carbonate-based solvents, ethylene carbonate (EC), and ethyl methyl carbonate (EMC), containing $LiPF_6$ salt in the desired concentration (adjusted to be 1.0M in all of the electrolytes) were purchased from Novolyte Industries, Inc. with less than 50 ppm of water. Mono-fluoroethylene carbonate (FEC) was also obtained from Novolyte and blended with stock electrolyte solutions. Bis (2,2,2-trifluoroethyl)(DTFEC, or BTFEC) carbonate and 2,2,2-trifluoroethyl methyl carbonate (TFEMC) were synthesized and purified at the University of Southern California using known techniques. (16) Triphenyl phosphate (TPP) was obtained from Sigma-Alrich Chem. Co., and used as received.

The electrical characterization of the three-electrode cells (i.e., charge-discharge measurements and cycling tests) was performed with an Arbin battery cycler. The cycling tests were generally performed at current densities of 0.25 mA/cm^2 (~ C/16 rate) and 0.50 mA/cm^2 (~ C/8 rate) for charge and discharge, respectively. The cells were charged to 4.10V, followed by a tapered charge period at constant potential, and discharged to 2.75V, with 15 minutes of interval between the charge/discharge steps. To maintain the cells at the desired temperature, they were placed in Tenney environmental chambers (+/− 1°C). After performing initial discharge characterization at various temperatures, the cells were either subjected to cycling at ambient temperature (100 cycles) or limited cycling at high temperature (i.e., 20 cycles at 60°C, and in some cases 80°C) followed by electrochemical

characterization. After completing this characterization, the electrodes were harvested from the cells for ex-situ analysis at Hunter College.

For NMR measurements, the electrodes (both anode and cathode) were rinsed in DMC to remove residual electrolyte and then scraped off the current collectors. Each sample was packed into 1.6 mm rotors. All manipulations were carried out inside an argon filled glove-box. NMR measurements were carried out on a Varian Direct Digital Drive NMR spectrometer with a 7.1T magnetic field strength and an MAS rate of 39 kHz. Aqueous lithium triflate (lithium trifluoromethanesulfonate) solution was used as the chemical shift reference for ^{7}Li and $CFCl_3$ was used for ^{19}F. A spin echo sequence with a 1.1 μs $\pi/2$ pulse width and 10s recycle delay was employed for ^{7}Li and ^{19}F measurements. The same pulse sequence was used for ^{31}P MAS NMR with a recycle delay of 200s. ^{31}P chemical shifts were referenced to an 85% H_3PO_4 aqueous solution. Accumulation of about 50 transients for both^{7}Li and ^{19}F MAS NMR were sufficient, the other hand, due to low signal-to-noise, ^{31}P MAS NMR measurements were signal averaged for longer periods of time (~48 hours).

Results

The ^{7}Li MAS NMR spectra of several cathodes, each one labeled by its electrolyte formulation, are illustrated in Fig 1. The spectrum for the “baseline” cell prepared with a standard electrolyte appears at the bottom. The peak around zero ppm is attributed to irreversible lithium contained in the SEI and some dried electrolyte salt (11). The broad feature centered at around 200 ppm arises from Li^+ ions in the active cathode material. This relatively large shift is attributed to the presence of paramagnetic Ni^{3+} in the cathode. The integrated area under the peak at 0 ppm is a measure of their reversible Li content in the cathode, and by such indication, the FEC+EMC+TPP sample exhibits the lowest irreversible content while the EC+EMC+TPP has the highest. Beyond these extremes, the accuracy of spectral integration of all compositions is limited by the uncertain amount of residual $LiPF_6$ and the relatively large line width of the paramagnetically shifted peak.

Another notable feature of the spectra in Fig. 1 is the variation of shift value of the center of the active cathode peak, which is attributed to differences in Ni^{3+}/Ni^{4+} ratio (Ni^{4+} is diamagnetic). Because this ratio is directly related to the state of charge (SOC) at the time that the cell was disassembled, it is possible, in principle, to compare this to the electrochemical SOC. If discrepancies between the two kinds of SOC values, which will be presented elsewhere, are noted, this information could be used to determine the degree of particle isolation, whereby certain regions of the cathode are no longer accessible to the cell (17).

^{7}Li MAS NMR of the harvested anodes corresponding to the cathodes described above are displayed in Fig. 2. The “baseline” anode spectrum is at the bottom. Again, similar to the cathode, the peak around zero ppm is attributed to Li residing in the SEI and the dried electrolyte salt. However, the line-widths are much larger than the corresponding signal (centered around zero ppm) in the cathodes. Although the cells were assumed to be fully discharged, the small feature around 45 ppm of the EC, EMC, TFEMC, TPP sample is indicative of a small amount of stage-1 intercalated lithium (11). The overlapped peak

around 8 ppm might be a contribution from a higher stage intercalated lithium (11). In the other spectra, except for the EC, EMC, TPP one, these features are unresolved and are most likely broadened by a distribution of unidentified Li compounds.

^{19}F MAS NMR spectra cathode materials are shown in Fig. 3. These data appear very similar, yet there are notable differences. The peak around −75 ppm is assigned to $LiPF_6$ (11, 18) in the dried electrolyte and the one at −205 ppm is attributed to LiF (11). The resonances of the PVdF binder appear around −90ppm and −113ppm (11). LiF has previously been identified as an SEI component that is deleterious to performance (4,5, 11, 13–15). A small peak, around −184ppm is presently unassigned. The highest LiF content is found in the EC, EMC, TPP cathode.

^{19}F MAS NMR spectra of the anodes are displayed in Fig. 4. The $LiPF_6$ peak around −75ppm is clearly present in most of the samples (the apparent large feature near this value is due to overlap with a spinning sideband in EC, EMC, TPP) but the PVdF peaks around −90ppm and −113ppm are severely broadened. This broadening is particularly noticeable in the samples prepared with fluorinated carbonates. Because it is known that CF_3 groups resonate in the region of ~−50 to −80 ppm (19) it is surmised that some of the electrolyte breakdown products detected by NMR originate in the fluorinated carbonates. However, what is most striking is that the anodes exhibit a higher a much higher LiF concentration than the cathodes, relative to the PVdF signal, and this is particularly the case for the EC +EMC+TPP sample. The spectral structure in the region of the $LiPF_6$ resonance is affected by the overlap of an LiF spinning side band in this sample and to a lesser extend all of the other anodes.

^{31}P MAS NMR spectra of the cathode series are shown in Fig. 5. Although the spectra were signal averaged for about 48 hours, the signal to noise is still quite low compared to the ^{7}Li and ^{19}F spectra. However four resolvable peaks can be identified at 4, −4, −12 and −18 ppm and are all assigned to hydrolysis products of $LiPF_6$ (18). The peaks at −4 and −12 ppm are assigned to PO_3F^{2-} and the peak at −18ppm is assigned to $PO_2F_2^-$ (18).The 4 ppm peak is currently unassigned. No resolved signals were observed between −133 and −156 ppm where $LiPF_6$ is known to resonate (18), but this is attributed to the generally low signal to noise ratio of the ^{31}P spectra. Beyond these resonances, there is additional spectral intensity in the samples prepared with TPP compared to the baseline electrolyte. This implies the presence of TPP decomposition products resulting from the aging protocol.

^{31}P MAS NMR spectra of the anode series are illustrated in Fig. 6. The rather large linewidths and lack of resolved splittings imply a broad and heterogeneous distribution of phosphorus-containing compounds in the anodes, compared to the cathodes. Only the $PO_3F_2^-$ peak at −12 ppm is resolvable; the other peaks overlap within the broad spectra. A set of features around −150 ppm appears only in the EC, EMC, TPP sample and is assigned to $LiPF_6$, which is consistent with the relatively large ^{19}F signal associated with $LiPF_6$ in the same sample shown in Fig. 4. On the anode side, the effect of possible TPP decomposition on the ^{31}P NMR spectra is not easily discernible, as it is on the cathode side.

Discussion and Conclusions

Electrochemical reactions occurring inside a Li ion cell, especially under accelerated aging, extend to all of the electrolyte components including additives that are intended to enhance performance (operating voltage, lower flammability, etc). Solid State NMR offers a means to examine the ultimate fate of some of the electrolyte decomposition products that accumulate in the SEIs at both electrodes. These products may originate from the usual $LiPF_6$ hydrolysis and partial polymerization of organic carbonates processes reported in the literature or from decomposition of the additives themselves. In this work, it is demonstrated that on the cathode side there are differing amounts of irreversible Li and differing average SOC values for the same nominal electrochemical SOC at cell disassembly, and that some level of TPP decomposition and deposition on the electrode particles occurs. LiF is also observed to varying degrees. The main results for the anode side are, again, the observation of varying amounts of LiF, but to a far greater extent than on the cathode, and the presence of chemical species with CF_3 groups originating from the fluorinated carbonates. Correlation of these results with electrochemical data gathered just prior to cell disassembly is expected to yield valuable information on the specific role that the SEI in standard and advanced electrolyte cells plays in electrochemical performance. This task is underway and will be presented elsewhere.

Acknowledgments

The work at Hunter College was supported by the U.S. Department of Energy Office of Basic Energy Sciences, Grant No. DE-SC0005029. An NMR facility infrastructure grant from the National Institutes of Health, Grant No. RR 003037, is also acknowledged. The portion of the work carried out at the Jet Propulsion Laboratory, California Institute of Technology, was performed under contract with the National Aeronautics and Space Administration (NASA) and under sponsorship of the NASA-Exploration Systems Mission Directorate (ESRT) and the Department of Energy (BATT Program-LBNL).

References

1. Goodenough J and Kim Y, Chem. Mater, 22, 587 (2010).
2. Peled E, J. Electrochem. Soc, 126, 2047 (1979).
3. Aurbach D, J. Power Sources 119, 497 (2003).
4. Edstrom K, Gustafsson T, and Thomas J, Electrochim. Acta 50, 397 (2004).
5. Araki K and Sato N, J. Power Sources 124, 124 (2003).
6. Smart MC, Ratnakumar BV, Surampudi S, Prakash GKS, Hu J, and Cheung I, J. Power Sources, 119–12, 359–367 (2003).
7 (a). Sasaki Y, Takehara M, Watanabe S, Nanbu N, and Ue M., J. Fluorine Chem, 125, 1205–1209 (2004);(b)Nanbu N, Watanabe S, Takehara M, Ue M, and Sasaki Y, J. Electroanal. Chem, 625, 7–15 (2009).
8. Hyung YE, Vissers DR, Amine K, J. Power Sources, 119–121, 383 (2003)
9. Xu K, Ding MS, Zhang S, Allen JL, Jow TR, J. Electrochem. Soc 149, A622 (2002).
10. Wang YF, Guo XD, Greenbaum S, Liu J, and Amine K, Electrochem. Solid-State Lett, 4, A68 (2001).
11. Meyer B, Sakamoto S, Greenbaum SG, Grey CP, Electrochem. Sol. State Lett 8 A145 (2005).
12. Leifer N, Smart MC, Prakash GKS, Gonzalez L, Sanchez L, Grey CP, and Greenbaum J SG. Electrochem. Soc, 158, A471 (2011).
13. Dupre N, Cuisinier M, and Guyomard D, ECS Interface 20, 61 (2011).

14. Murakami M, Yamashige Y, Arai H, Uchimoto Y, and Ogumi Z, Electrochem. Solid-State Lett,14, A134 (2011).

15. Leifer ND and Greenbaum SG, in Advanced Materials and Methods for Lithium-Ion Batteries, Zhang SS, ed., Ch.16, Research Signpost (2007).

16 (a). Hu J, Ph.D. Dissertation, University of Southern California, 2002.;(b)Krespan CG and Smart BE, J. Org. Chem, 51, 320 (1986).

17. Kerlau M, Reimer JA, Cairns EJ, *Electrochem. Comm.* 7, 1249 (2005).

18. Plakhotnyk AV, Ernst L, Schmutzler R, J. Fluorine Chem 126, 27 (2005).

19. Bruker Biospin Almanac, p.14 (2003).

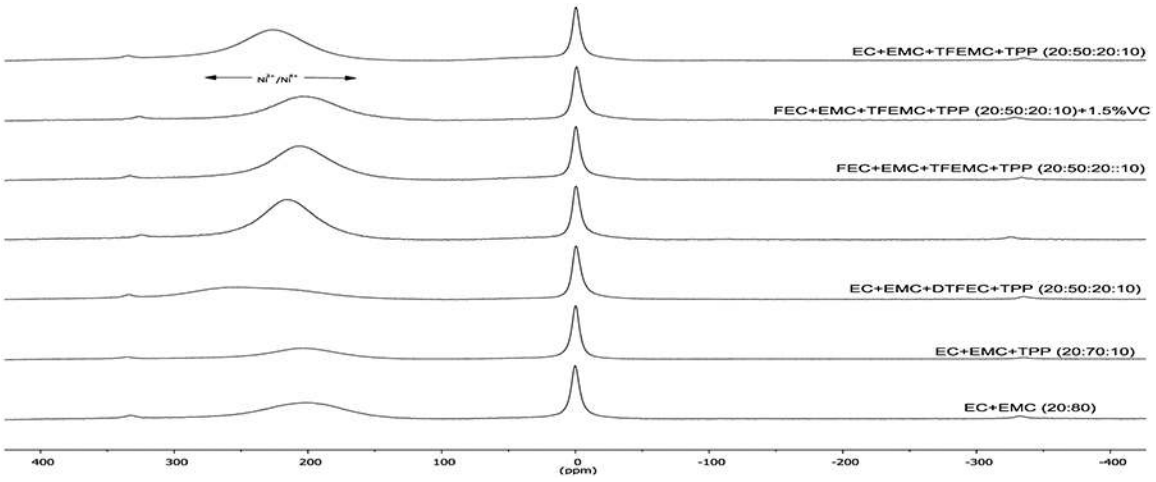

Figure 1.

^{7}Li MAS NMR spectra of $LiNi_{0.8}Co_{0.2}O_2$ cathode material harvested from cycled cells, with electrolyte formulations indicated. The baseline compound appears at the bottom.

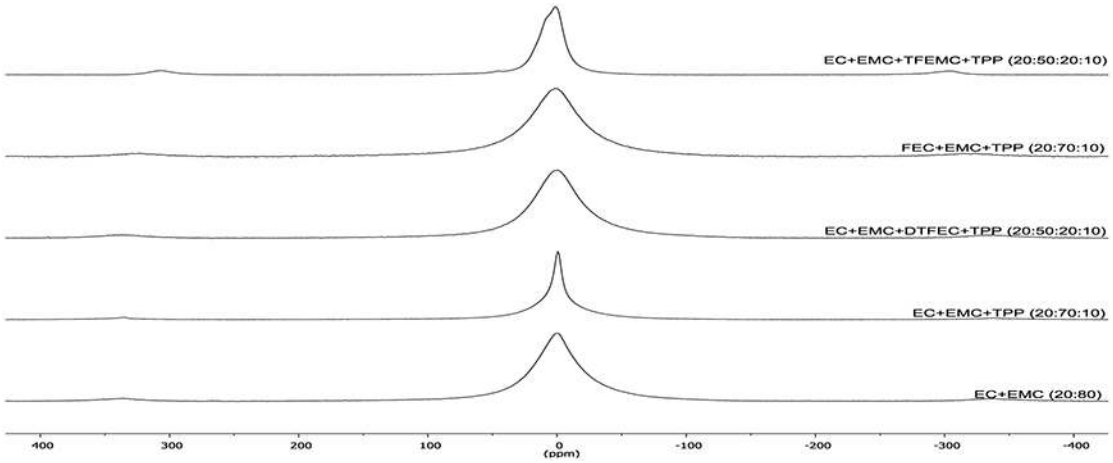

Figure 2.

^{7}Li MAS NMR spectra of MCMB anode material harvested from cycled cells, with electrolyte formulations indicated. The baseline compound appears at the bottom.

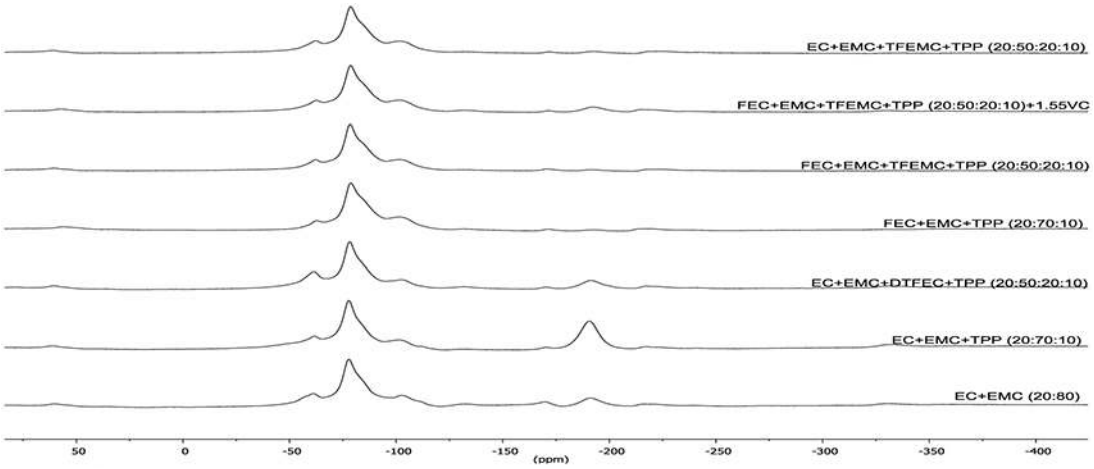

Figure 3.

^{19}F MAS NMR spectra of $LiNi_{0.8}Co_{0.2}O_2$ cathode material harvested from cycled cells, with electrolyte formulations indicated. The baseline compound appears at the bottom.

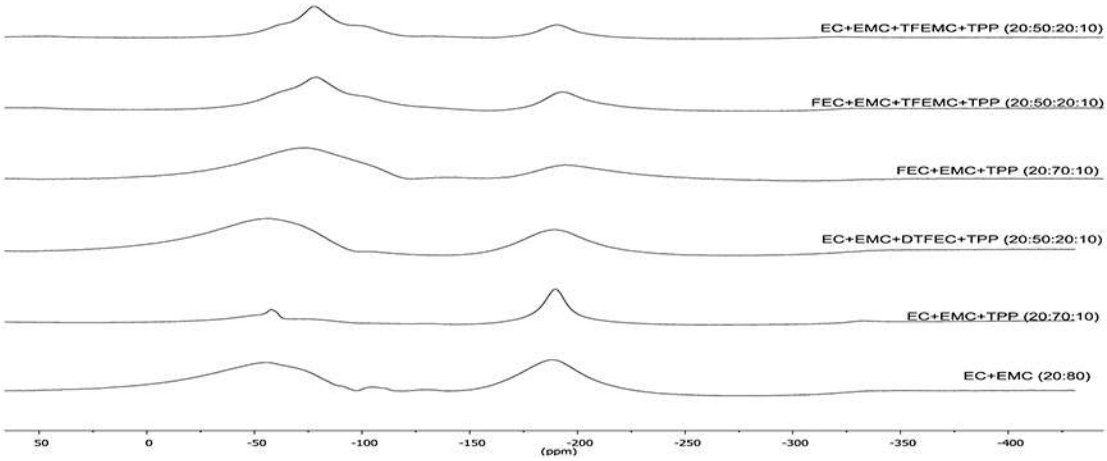

Figure 4.

^{19}F MAS NMR spectra of MCMB anode material harvested from cycled cells, with electrolyte formulations indicated. The baseline compound appears at the bottom.

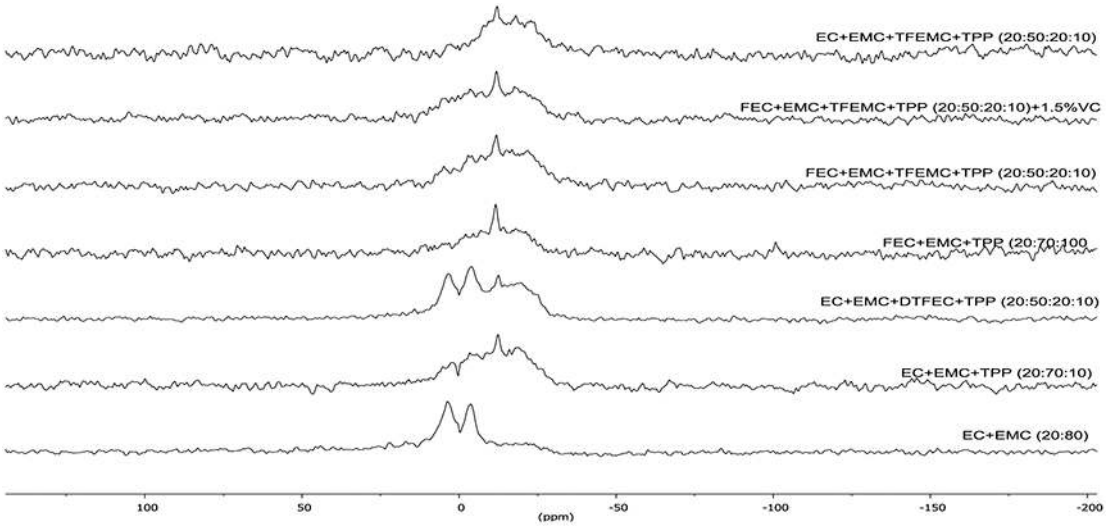

Figure 5.

^{31}P MAS NMR spectra of $LiNi_{0.8}Co_{0.2}O_2$ cathode material harvested from cycled cells, with electrolyte formulations indicated. The baseline compound appears at the bottom.

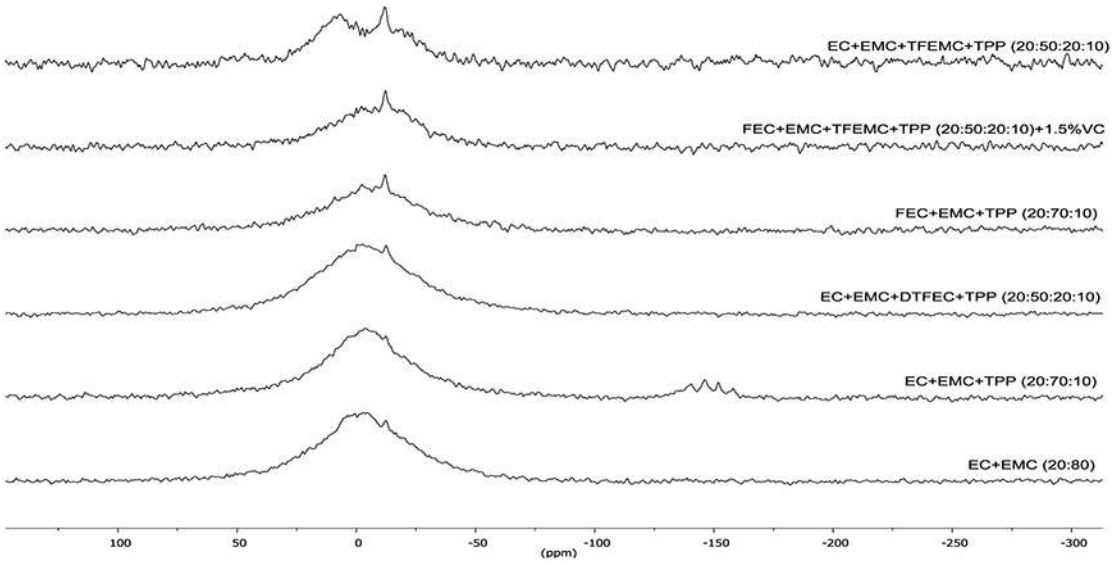

Figure 6.

^{31}P MAS NMR spectra of MCMB anode material harvested from cycled cells, with electrolyte formulations indicated. The baseline compound appears at the bottom.